PHYSICAL REVIEW A, VOLUME 64, 042705

Exact exchange effects on vibrational excitation of H_2 by electron impact

K. T. Mazon and R. Fujiwara
Departamento de Física, UFSCar 13565-905 São Carlos, São Paulo, Brazil

M.-T. Lee
Departamento de Química, UFSCar 13565-905 São Carlos, São Paulo, Brazil

(Received 18 April 2001; published 12 September 2001)

A representation of the exact nonlocal exchange-potential operator is proposed and applied to study electron-impact vibrational excitation of H_2 in the low- and intermediate-energy range. In our approach, a complete set of one-dimensional particle-in-box wave functions is used as expansion basis. This representation of the exchange operator is easy to program and the calculated cross sections converge rapidly with the number of basis functions. Excitation cross sections for the transitions $v'=0\rightarrow v=0$, 1, 2, and 3 calculated in the 1.5–100-eV range are in general good agreement with the available experimental and theoretical data.

DOI: 10.1103/PhysRevA.64.042705 PACS number(s): 34.80.Bm

I. INTRODUCTION

During the past three decades, considerable activities on theoretical studies of electron-impact vibrational excitation of molecules were reported in the literature [1–8]. The body-frame vibrational close-coupling (BFVCC) approach [2,4], which incorporates vibrational effects exactly, has been widely applied for these studies. In this approximation, rotational levels of molecules are treated as essentially degenerated, which reduces significantly the number of coupled equations. Consequently, computational efforts for electron-impact vibrational-excitation studies are also significantly reduced. Despite that, taking correctly the nonlocal exchange effect into account in calculations of vibrational-excitation cross sections is still a very difficult task. Most investigations reported in the literature made use of some model exchange potentials [9–11]. Among them, the so-called "tuned free-electron-gas exchange" (TFEGE) potential proposed by Morrison and Collins [11] is the most successful. TFEGE is an approximate free-gas local exchange potential based on the familiar Hara's model [9]. The essence of the TFEGE is to treat the internuclear-distance-dependent ionization potential, $I(R)$, used to determine the local momentum of the scattering electron, as a theoretical parameter. The determination of the quantity $I(R)$ is based entirely on theoretical considerations. For instance, at each internuclear distance and for each incident energy, it is obtained from adjustment to an eigenphase sum calculated using the exact static-exchange (ESE) approach for a determined scattering channel.

Recently, we applied the method of continued fractions (MCF) [12] in calculations of electron-impact vibrational-excitation cross sections of H_2 in the low-incident-energy range. An optical potential formed by static, exchange, and correlation-polarization contributions was used to represent the collisional dynamics. The TFEGE model potential with $I(R)$ determined by adjusting the eigenphase sum of the $^2\Sigma_g$ scattering channel to that obtained in an ESE calculation were used in that study. Although in general, the calculated cross sections of that study for the vibrational elastic collisions are in good agreement with experimental data and with some recent calculated results available in the literature, at some impact energies discrepancies between calculated and experimental results were seen for vibrational-excitation cross sections. Moreover, such discrepancies became more significant for excitations leading to higher vibrational states. The use of the approximate TFEGE potential was attributed as the origin of these discrepancies.

In the present work, we propose a representation for the exact exchange-potential operator. A complete set of one-dimensional particle-in-box wave functions is used as expansion basis. Results of the application of this exchange operator to study electron-impact vibrational excitations of H_2 will also be presented.

The organization of this article is as follows. In Sec. II, we briefly outline the theory used. The comparison of our calculated results with available data is presented in Sec. III, where we also give some concluding remarks.

II. THEORY AND CALCULATION

The laboratory-frame (LF) differential cross sections (DCS) averaged over the molecular orientations, for vibrational excitation from an initial vibrational level v to a final level v', is expressed in the j_t-basis representation [13] as

$$\frac{d\sigma}{d\Omega}(v\rightarrow v')=\frac{k_f}{k_0}\sum_{j_t m_t m_t'}\frac{1}{(2j_t+1)}\times|B^{j_t}_{m_t m_t'}(v\rightarrow v',k_0,k_f,\hat{r}')|^2, \tag{1}$$

where $\vec{j}_t=\vec{l}'-\vec{l}$ is the transferred angular momentum during the collision, while m_t' and m_t are the projections of j_t along the laboratory and molecular axis, respectively. The k_0 and k_f are the momenta of the incoming and the outgoing electron, respectively. In Eq. (1), $B^{j_t}_{m_t m_t'}(v\rightarrow v')$ are coefficients of the j_t-basis expansion of the LF vibrational-excitation scattering amplitudes and is given by

$$B^{j_t}_{m_t m_t'}(v \rightarrow v',\Omega') = \sum_{l'lm'm} (-1)^m a_{ll'mm'}(ll'0m_t|j_t m_t) \times (ll'mm'|j_t m_t')Y_{lm_l}(\Omega'), \quad (2)$$

where the dynamical coefficients $a_{ll'mm'}$ for the transition from an initial vibrational state $|v\rangle$ to a final state $|v'\rangle$ are related to the partial-wave components of the vibrational-excitation transition-matrix elements as

$$a_{ll'mm'}(v \rightarrow v') = -(1/2)\pi[4\pi(2l'+1)]^{(1/2)} i^{l'-l} \times \langle k_f lm, v'|T|k_0 l'm', v\rangle. \quad (3)$$

In the present work, the reactance K matrices were calculated by solving the BFVCC scattering equations,

$$(\boldsymbol{\nabla}^2 + k_{v'}^2)F_{v'} = \sum_v U_{v'v}F_v, \quad (4)$$

where $F_{v'}$ is the wave function of the scattering electron associated with the target vibrational state $|v'\rangle$, $k_{v'}^2$ is the kinetic energy of the scattered electron in Rydbergs, and $U_{v'v}$ is the vibrational-excitation interaction-potential operator.

In the present work, a set of coupled equations are solved using the MCF. The MCF, originally proposed by Horáček and Sasakawa [14] for single-channel electron-atom scattering, has been extended by our group to treat actual electron-molecule-scattering problems. Recently we have satisfactorily applied the MCF to the calculation of elastic- and electronic-excitation cross sections for electron scattering by H_2 in the low- and intermediate-energy range [15–18].

Equation (4) can be converted into a Lippmann-Schwinger integral equation, in matrix form,

$$\tilde{\Psi} = \tilde{S} + \tilde{G}_0\tilde{U}\tilde{\Psi}, \quad (5)$$

where $\tilde{\Psi}$ is the solution of Eq. (5) in matrix form, $\tilde{S}$ is a diagonal matrix that represents a set of solutions of the unperturbed Schrödinger equation, $\tilde{G}_0$ is also a diagonal matrix that represents the unperturbed Green's operator, and $\tilde{U}$ is the potential-operator matrix.

The application of MCF consists basically of defining the nth-order *weakened* potential operator $\tilde{U}^{(n)}$ as

$$\tilde{U}^{(n)} = \tilde{U}^{(n-1)} - \tilde{U}^{(n-1)}|\tilde{S}^{(n-1)}\rangle(\tilde{A}^{(n-1)})^{-1}\langle\tilde{S}^{(n-1)}|\tilde{U}^{(n-1)} \quad (6)$$

and the nth-order correction of $\tilde{D}$ matrix is defined through the relation

$$\tilde{D}^{(n)} = \tilde{B}^{(n)} + \tilde{A}^{(n)}[\tilde{A}^{(n)} - \tilde{D}^{(n+1)}]^{-1}\tilde{A}^{(n)}. \quad (7)$$

Here,

$$\tilde{A}^{(n)} = \langle\tilde{S}^{(n)}|\tilde{U}^{(n)}|\tilde{S}^{(n)}\rangle, \quad (8)$$

$$\tilde{B}^{(n)} = \langle\tilde{S}^{(n-1)}|\tilde{U}^{(n-1)}|\tilde{S}^{(n)}\rangle, \quad (9)$$

where

$$\tilde{S}^{(n)} = \tilde{G}_0^P\tilde{U}^{(n-1)}\tilde{S}^{(n-1)} \quad (10)$$

and $\tilde{G}^P$ denotes the principal-value unperturbed Green's operator. The scattering $\tilde{K}$ matrix is related with the $\tilde{D}$ matrix via

$$\tilde{K} = -\tilde{D}. \quad (11)$$

$\tilde{U}^{(n)}$, defined in Eq. (6), is expected to become weaker and weaker with increasing n. As a result, the iterative procedure can be stopped after some steps when the desired convergence is achieved. The converged $\tilde{K}$ matrix would correspond to what can be obtained through the exact solution of the scattering equation (5). In practice, the nth-order $\tilde{D}$-matrix can be obtained using Eq. (7) by setting $D^{(n+1)} = 0$. Repeating the procedure of Eq. (7), one obtains backwardly $\tilde{D}^{(n-1)}$, $\tilde{D}^{(n-2)}$, . . . ,$\tilde{D}^{(1)}$ and $\tilde{D}$. The nth-iteration $\tilde{K}$ Matrix is calculated via Eq. (11).

The transition matrix is given by

$$\tilde{T} = -\frac{2\tilde{K}}{(1 - i\tilde{K})}. \quad (12)$$

The electron-molecule-interaction potential for low-energy vibrational excitation is formed by three main components, viz.,

$$V^{int}(\vec{r},R) = V^{st}(\vec{r},R) + V^{cp}(\vec{r},R) + V^{ex}(\vec{r},R). \quad (13)$$

The static potential $V^{st}(\vec{r},R)$ is the electrostatic term arising from Coulomb interactions between the projectile and the nuclei and electrons of the target. In this study, the R-dependent V^{st} was derived exactly from the target wave functions. They were calculated for 15 internuclear distances varying from 0.6 to 3.5 au. At each distance, the ground-state target wave function was calculated within the Hartree-Fock self-consistence-field (SCF) framework. These wave functions were constructed with a $5s/3p$ uncontracted Cartesian Gaussian basis set of Huzinaga [19] augmented by three s- ($\alpha = 0.04$, 0.015, and 0.005) uncontracted functions. With this basis set, the calculated SCF energy for the ground-state H_2 at the equilibrium internuclear distance (1.4006 a_0) is $-1.133\,022$ a.u., to be compared with the Hartree-Fock limit of -1.1336 a.u. [20].

The V^{cp} appearing in Eq. (13) is the correlation-polarization potential arising at short range from bound-free many-body effects and at long range from induced-polarization effects. Strictly speaking, the V^{cp} is also nonlocal and depends on the scattering energy. In the present work, this contribution is approximated by a parameter-free local potential as prescribed by Padial and Norcross [21]. The published R-dependent dipole polarizabilities of H_2 [22] are used to describe the asymptotic form of the V^{cp}.

The third term in the right-hand side of Eq. (13) is a nonlocal energy-dependent exchange contribution arising from the antisymmetric consideration between the scattering and target electrons. This nonlocal contribution to the transition $|v'\rangle \rightarrow |v\rangle$ can be written as a kernel,

$$V^{ex}_{v'v}F_v(\vec{r}) = \langle \chi_{v'}(R)\phi(\vec{r}_i;R)| \frac{1}{|\vec{r}-\vec{r}_i|} |F_v(\vec{r}_i)\phi(\vec{r};R)\chi_v(R)\rangle, \tag{14}$$

where $\phi(\vec{r}_i;R)$ are the R-dependent ground-state electronic wave function of the target, $\chi_v(R)$ are the vibrational wave functions, $\vec{r}_i$ denotes collectively the position of all target electrons, the integrals are performed over the $\vec{r}_i$ and the internuclear distance R. In principle, the direct calculation of this kernel is possible. However, the formidable computational efforts required for this calculation makes it unfeasible. In order to overcome these difficulties, a separable potential approximation is used in this work. We have made use of the closure property of a complete set of orthonormal functions,

$$\sum_n |n\rangle\langle n| = 1. \tag{15}$$

Therefore, the kernel of Eq. (14) can be rewritten as

$$V^{ex}_{v'v}F_v(\vec{r}) = \sum_n \langle \phi_{v'n}(\vec{r}_i)| \frac{1}{|\vec{r}-\vec{r}_i|} |F_v(\vec{r}_i)\phi_{nv}(\vec{r})\rangle, \tag{16}$$

where

$$\phi_{vn} = \langle \chi_v(R)|\phi(\vec{r}_i;R)|n(R)\rangle. \tag{17}$$

In the present study, the one-dimensional particle-in-box wave functions

$$\Psi_n = \left(\frac{2}{b}\right)^{1/2} \sin\left(\frac{n\pi[R-R_0]}{b}\right) \tag{18}$$

are used to generate the exchange kernel. In Eq. (18), b is the size of the box and R_0 is the minimum internuclear distance used in the calculation. In the present study, 25 basis functions are used to represent the exchange operator leading to the convergence of calculated cross sections to be better than 0.2%.

Finally, in order to calculate the vibrational-excitation interaction-potential matrix elements $U_{v'v}$, the vibrational wave functions $\chi_v(R)$ were calculated using the numerical method of Cooley [23] from the Rydberg-Klein-Rees (RKR) potential curve of the ground electronic state H_2 [24]. These wave functions were calculated in a 801-point grid, covering the $0.6 \leqslant R \leqslant 3.5$ a.u. range. The R-dependent interaction potentials defined in Eq. (13) were interpolated over the same grid and the integral over this internuclear-distance grid was evaluated using the Simpson's rule.

The number of vibrational states that must be included for solving the BFVCC scattering equation, Eq. (4), depends on the incident energy, especially on whether the scattering is resonant or nonresonant. In the energy range covered herein, it required four vibrational states to converge the reported elastic and excitation cross sections to better than 2%.

III. RESULTS AND DISCUSSIONS

Figures 1–3 show the calculated DCS for the vibrational-elastic ($v=0 \rightarrow v'=0$) electron-H_2 collisions at 1.5, 2.5, 4.5, 6, 10.8, and 20 eV incident energies along with some experimental data available in the literature [25–28]. Results of Lee *et al.* [12] calculated using a local TFEGE-model exchange potential are also shown for comparison. In general, there is a good agreement between the calculated and measured data in the entire energy range covered herein. In addition, the vibrationally elastic DCS calculated using the exact and approximated exchange potentials also agree very well with each other indicating that the TFEGE model potential is a good approximation for elastic electron-H_2 scattering.

In Figs. 4 and 5 we present our calculated vibrational-excitation ($v=0 \rightarrow v'=1$) DCS for electron-H_2 scattering at 1.5, 2.5, 4.5, and 45 eV incident energies. Experimental results available in the literature [25,27,29,30] as well as the calculated data using the TFEGE model [12] are also shown for comparison. In general, the present calculated results are in very good agreement with the measured data, both qualitatively and quantitatively. The comparison between the present data and results calculated using the TFEGE also show a good qualitative agreement. However, the quantitative agreement between them is fair at lower incident energies indicating that the vibrational-excitation

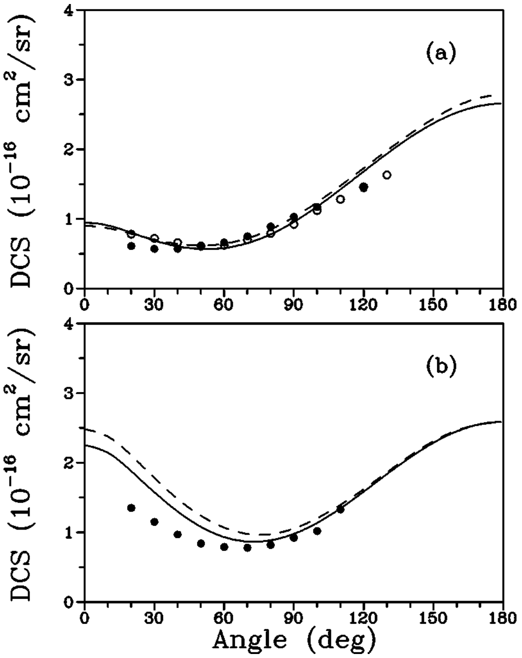

FIG. 1. DCS for vibrationally elastic electron-H_2 scattering at (a) 1.5 eV and (b) 2.5 eV incident energies. Solid line presents calculated results with exact exchange potential; dashed line, calculated results with TFEGE [12]; full circles, measured data of Linder and Schmidt [25]; open circles, measured data of Brunger *et al.* [26].

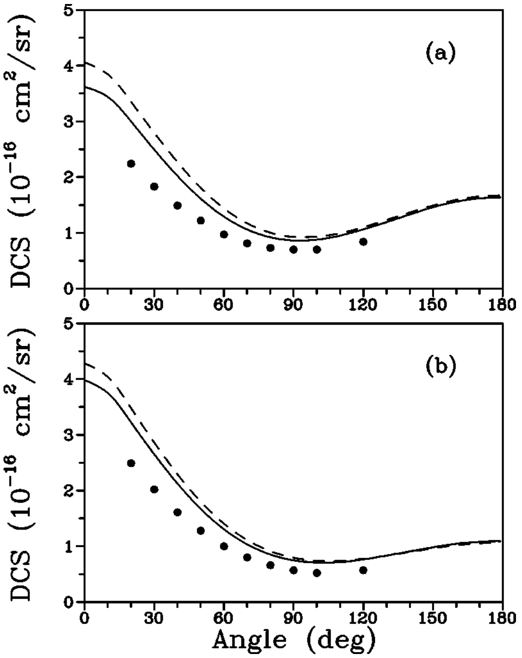

FIG. 2. Same as Fig. 1 but for (a) 3.5 eV and (b) 6 eV.

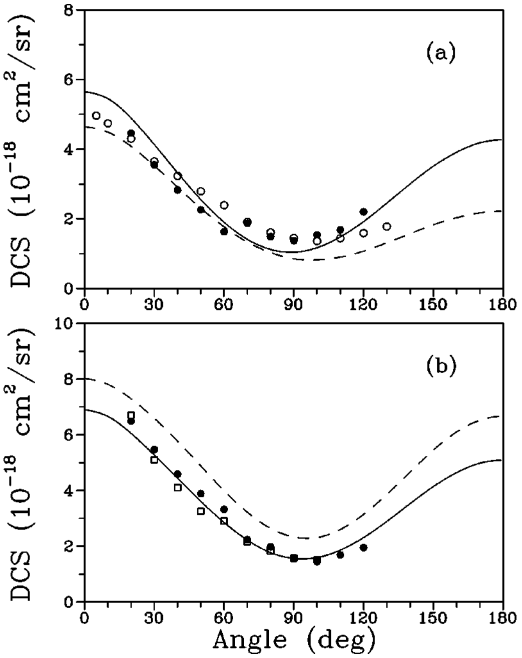

FIG. 4. DCS for vibrational ($v=0\rightarrow v'=1$) excitation of H_2 by electron impact at (a) 2.5 eV and (b) 4.5 eV incident energies. The symbols used are the same as in Fig. 1 except open squares denote measured data of Wong and Schulz [30]. The experimental results of Wong and Schulz are obtained by summing up their DCS for the $\Delta J=0$ and $J=0\rightarrow J'=3$ rovibrational transitions.

cross sections are more sensitive to the exchange-interaction potential.

Figures 6 and 7 show our calculated DCS for the vibrational ($v=0\rightarrow v'=2$) transition in H_2 by electron impact along with the TFEGE data at 1.5, 2.5, 4.5 and 45 eV. The experimental data of Wong and Schulz [30] at 4.5 eV and Trajmar *et al.* [29] at 45 eV are also shown for comparison. The comparison of our results with the TFEGE data reveals that the calculated cross sections of this vibrational excitation are highly dependent on the quality of the description of exchange interactions. As expected, DCS calculated with the exact exchange are in better agreement with experimental

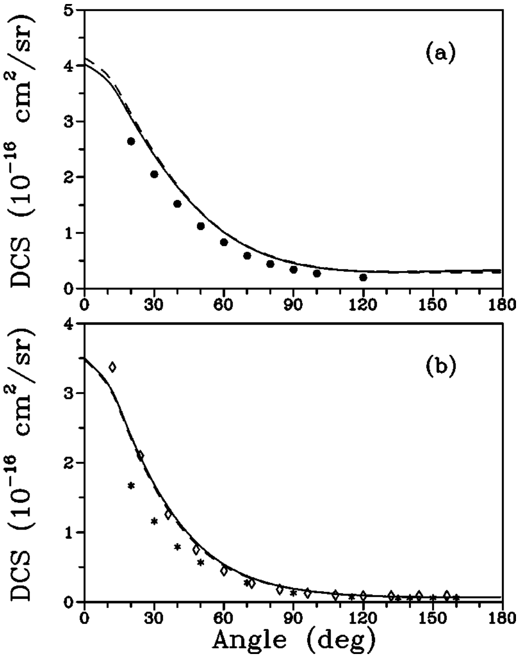

FIG. 3. Same as Fig. 1 but for (a) 10.8 eV and (b) 20 eV. Open diamond, experimental data of Shyn and Sharp [27]; stars, measured data of Srivastava *et al.* [28].

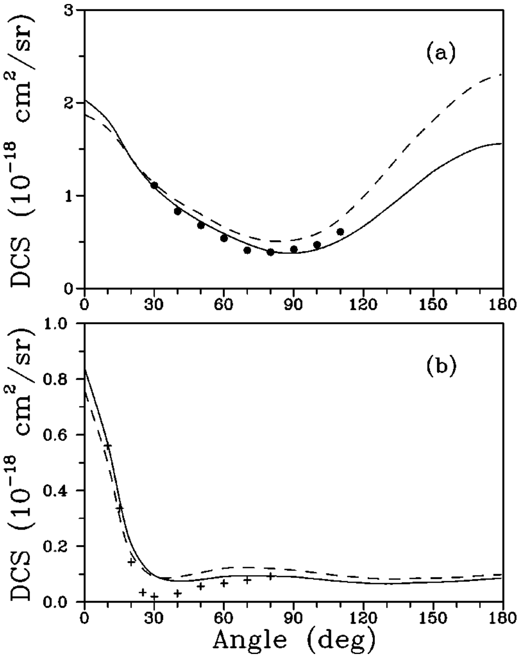

FIG. 5. Same as Fig. 4 but for (a) 10.8 eV and (b) 45 eV. Crosses, measured data of Trajmar *et al.* [29].

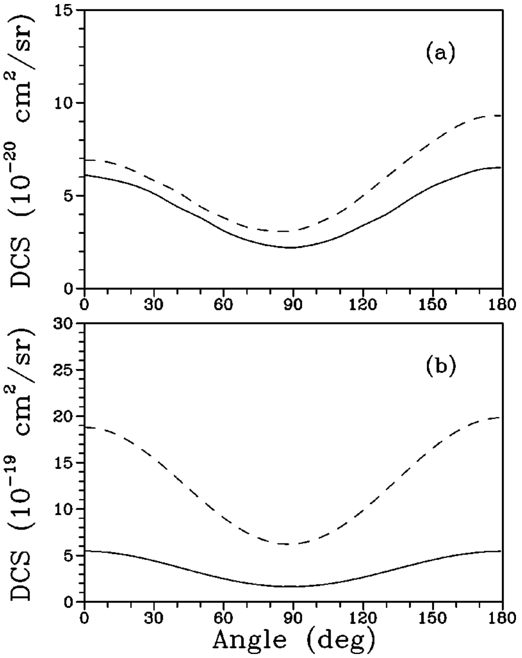

FIG. 6. Electron-impact DCS for vibrational $(v=0\rightarrow v'=2)$ transition in H_2 at (a) 2.5 eV and (b) 3.5 eV. The symbols used are the same as in Fig. 1.

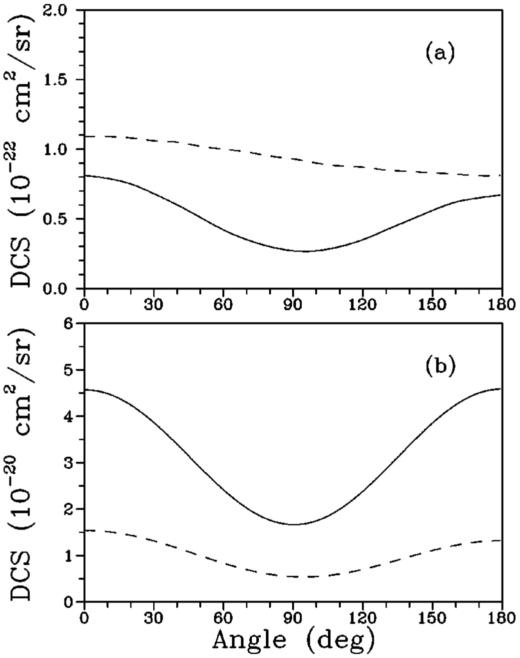

FIG. 8. Electron-impact DCS for vibrational the $(v=0\rightarrow v'=3)$ transition in H_2 at (a) 2.5 eV and (b) 3.5 eV. The symbols used are the same as in Fig. 6.

data at 4.5 eV than those of the TFEGE model. On the other hand, DCS calculated using both exchange approaches at 45 eV are in good agreement with each other.

In Figs. 8 and 9 we present our calculated DCS for electron-impact vibrational $(v=0\rightarrow v'=3)$ excitation of H_2 at 1.5, 2.5, 4.5, and 45 eV. The theoretical TFEGE data [12] as well as the measured data of Wong and Schulz [30] at 4.5 eV are also shown for comparison. As in the $(v=0\rightarrow v'=2)$ excitation, significant differences between the present calculated results and those of the TFEGE calculation reinforce the fact that the excitations leading to higher vibrational levels are very sensitive to the description of exchange interactions. Again, DCS calculated with the exact exchange

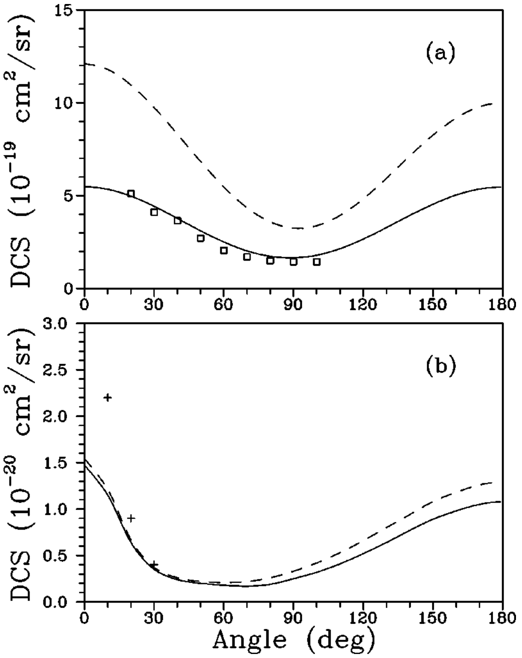

FIG. 7. Same as Fig. 6 but at (a) 4.5 eV and (b) 45 eV. Open squares, measured data of Wong and Schulz Ref. [30]; crosses, measured data of Trajmar *et al.* [29].

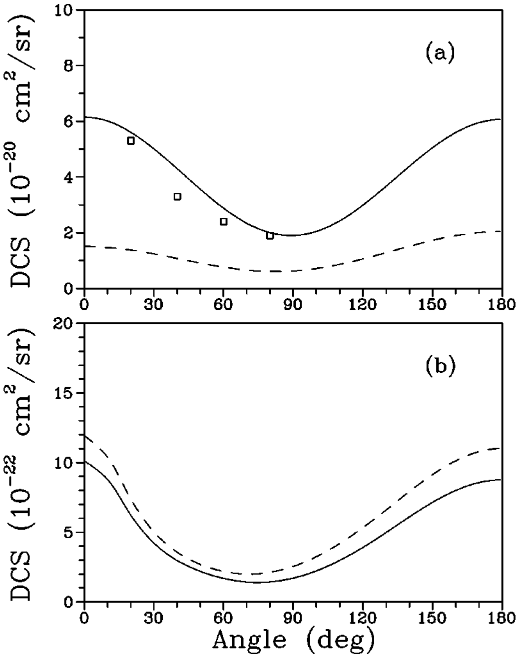

FIG. 9. Same as Fig. 6 but for (a) 4.5 eV and (b) 45 eV. The symbols used are the same as Fig. 7.

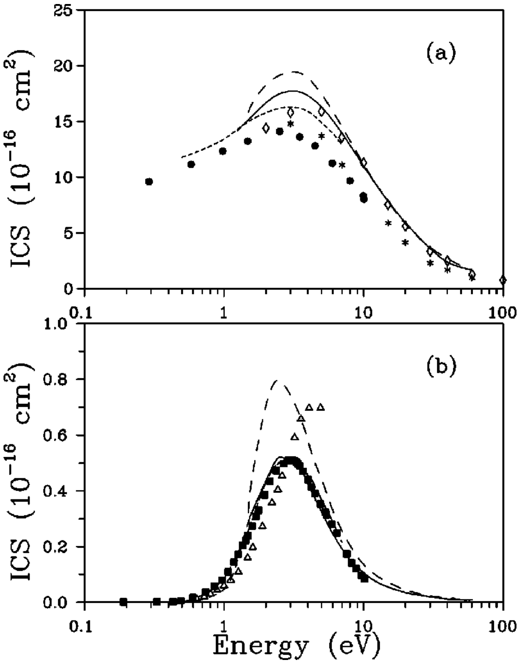

FIG. 10. ICS for (a) vibrationally elastic electron-H_2 scattering and (b) vibrational ($v=0 \rightarrow v'=1$) excitation of H_2 by electron impact. Solid line presents calculated results with exact exchange potential; dashed line, calculated results with TFEGE [12]; short-dashed line, the calculated results of Snitchler *et al.* [33]; full circles, measured data of Linder and Schmidt [25]; open diamonds, measured data of Shyn and Sharp (1981); stars, experimental results of Srivastava *et al.* [28]; full squares, experimental results of Ehrhardt *et al.* [31]; open triangles, experimental results of Gibson [32].

are in much better agreement with experimental data at 4.5 eV. On the other hand, even at incident energy as high as 45 eV, significant discrepancies are seen in the DCS calculated using the exact and approximated exchange operators.

Figure 10 compares our calculated integral cross sections (ICS) for the ($v=0 \rightarrow v'=0$ and 1) transitions in H_2 by electron impact with some available experimental data [25–27,31,32]. The TFEGE ICS and calculated results of Snitchler *et al.* [33] for the ($v=0 \rightarrow v'=0$, 1) transitions are also shown for comparison. The results of Snitchler *et al.* (1990) were also calculated using an exact exchange potential represented in a separable form. Bound and virtual molecular orbitals of the target were used as expansion basis in their representation. Generally, our calculated ICS with exact exchange potential are in very good agreement with the available experimental data for both vibrationally elastic and inelastic scatterings. They are also in good agreement with the calculated results of Snitchler *et al.* On the other hand, the calculation with TFEGE potential overestimates significantly the ICS near the maxima.

In Fig. 11, we show our calculated ICS for the ($v=0 \rightarrow v'=2$ and 3) transitions in H_2 by electron impact with the experimental data of Ehrhardt *et al.* [31] and with the calculated results using the TFEGE-model potential. Significant differences seen between the two calculated ICS clearly demonstrate the importance of accounting for accurate exchange effects into electron-impact excitation processes leading to higher vibrational states. As expected, our calculated ICS with exact exchange potential are in much better agreement with the available experimental data than those of TFEGE calculations.

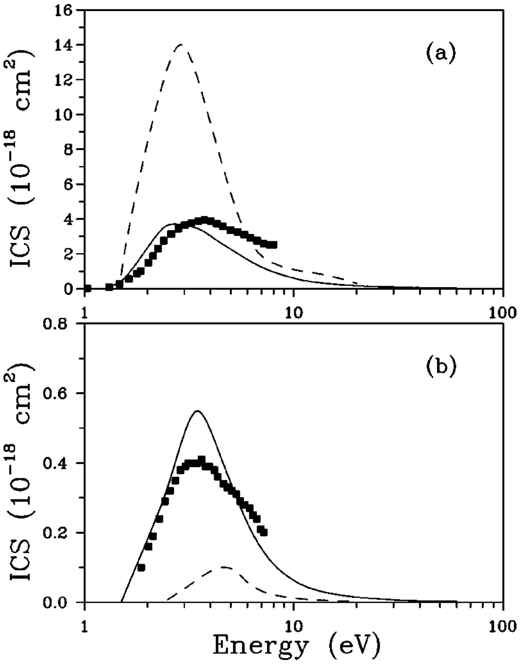

FIG. 11. Same as Fig. 10 but for (a) vibrational ($v=0 \rightarrow v'=2$) and (b) vibrational ($v=0 \rightarrow v'=3$) excitation of H_2 by electron impact.

In summary, from the present study one learns that the exchange effects play a very important role for the calculation of low-energy electron-impact vibrational-excitation cross sections, particularly, for those $v=0 \rightarrow v'=2$ and 3 transitions and therefore must be correctly accounted for. The representation of the exact exchange operator proposed here seems to be a very convenient manner for description of these effects. This representation made use of one-dimensional particle-in-box wave functions as expansion basis. Our study reveals that this is a very efficient manner and the calculated cross sections for vibrational ($v=0 \rightarrow v'=0$, 1, 2, and 3) transitions are very satisfactory when compared with the existing experimental and calculated data. One important advantage of this representation is the facility to be generalized to other molecular targets. Efforts in this direction is now in progress.

ACKNOWLEDGMENTS

This research was partially supported by Brazilian agencies FAPESP, CNPq, and FINEP-PADCT. R.F. thanks the FAPESP and K.T.M. thanks the CAPES for their financial support.

[1] R. J. W. Henry, Phys. Rev. A **2**, 1349 (1970).
[2] N. Chandra and A. Temkin, Phys. Rev. A **13**, 188 (1976).
[3] M. A. Morrison, A. N. Feldt, and D. Austin, Phys. Rev. A **29**, 2518 (1984).
[4] M. A. Morrison, A. N. Feldt, and B. C. Saha, Phys. Rev. A **30**, 2811 (1984).
[5] W. K. Trail, M. A. Morrison, W. A. Isaacs, and B. C. Saha, Phys. Rev. A **41**, 4868 (1990).
[6] M. A. Morrison, M. Abdolsalami, and B. K. Elza, Phys. Rev. A **43**, 3440 (1991).
[7] W. Sun, M. A. Morrison, W. A. Isaacs, W. K. Trail, D. T. Alle, R. J. Gulley, M. J. Brennan, and S. J. Buckman, Phys. Rev. A **52**, 1229 (1995).
[8] S. Mazevet, M. A. Morrison, O. Boydstun, and R. K. Nesbet, Phys. Rev. A **59**, 477 (1999).
[9] S. Hara, J. Phys. Soc. Jpn. **22**, 710 (1967).
[10] M. E. Riley and D. G. Truhlar, J. Chem. Phys. **63**, 2182 (1975).
[11] M. A. Morrison and L. C. Collins, Phys. Rev. A **23**, 127 (1981).
[12] M.-T. Lee, R. Fujiwara, K. T. Kahio, and M. M. Fujimoto, J. Mol. Struct.: THEOCHEM **541**, 51 (2001).
[13] U. Fano and D. Dill, Phys. Rev. A **6**, 185 (1972).
[14] J. Horáček and T. Sasakawa, Phys. Rev. A **28**, 2151 (1983).
[15] M.-T. Lee, M. M. Fujimoto, and I. Iga, J. Mol. Struct.: THEOCHEM **394**, 117 (1997).
[16] M.-T. Lee, M. M. Fujimoto, and I. Iga, J. Mol. Struct.: THEOCHEM **432**, 197 (1998).
[17] M.-T. Lee, M. M. Fujimoto, T. Kroin, and I. Iga, J. Phys. B **29**, L425 (1996).
[18] A. M. Machado, M. M. Fujimoto, A. M. A. Taveira, L. M. Brescansin, and M.-T. Lee, Phys. Rev. A **63**, 032707 (2001).
[19] S. Huzinaga, J. Chem. Phys. **42**, 1293 (1965).
[20] W. Kolos and C. C. J. Roothaan, Rev. Mod. Phys. **32**, 219 (1960).
[21] N. T. Padial and D. W. Norcross, Phys. Rev. A **29**, 1742 (1984).
[22] M. A. Morrison and B. C. Saha, Phys. Rev. A **34**, 2786 (1986).
[23] J. W. Cooley, Math. Comput. **15**, 363 (1961).
[24] R. J. Spindeler, Jr., J. Quant. Spectrosc. Radiat. Transf. **9**, 597 (1969).
[25] F. Linder and H. Schmidt, Z. Naturforsch. A **26A**, 1607 (1971).
[26] M. J. Brunger, S. J. Buckmann, D. S. Newman, and D. T. Alle, J. Phys. B **24**, 1435 (1991).
[27] T. W. Shyn and W. E. Sharp, Phys. Rev. A **24**, 1734 (1981).
[28] S. K. Srivastava, A. Chutjian, and S. Trajmar, J. Chem. Phys. **63**, 2659 (1975).
[29] S. Trajmar, D. G. Truhlar, J. K. Rice, and A. Kupperman, J. Chem. Phys. **52**, 4516 (1970).
[30] S. F. Wong and G. J. Schulz, Phys. Rev. Lett. **32**, 1089 (1974).
[31] H. Ehrhardt, D. L. Langhans, F. Linder, and H. S. Taylor, Phys. Rev. **173**, 222 (1968).
[32] D. K. Gibson, Aust. J. Phys. **23**, 683 (1970).
[33] G. Snitchler, S. Alston, D. K. Norcross, B. Saha, G. Danby, W. Trail, and M. A. Morrison (1990), as referred to by Brunger *et al.* in Ref. [26].